



HAL
open science

Comparison between voltage and current driving methods of a micro-speaker

E Sturtzer, Gaël Pillonnet, G Lemarquand, N Abouchi

► **To cite this version:**

E Sturtzer, Gaël Pillonnet, G Lemarquand, N Abouchi. Comparison between voltage and current driving methods of a micro-speaker. *Applied Acoustics*, 2012, 73, pp.1087 - 1098. 10.1016/j.apacoust.2012.05.008 . hal-01114019

HAL Id: hal-01114019

<https://hal.science/hal-01114019>

Submitted on 6 Feb 2015

HAL is a multi-disciplinary open access archive for the deposit and dissemination of scientific research documents, whether they are published or not. The documents may come from teaching and research institutions in France or abroad, or from public or private research centers.

L'archive ouverte pluridisciplinaire **HAL**, est destinée au dépôt et à la diffusion de documents scientifiques de niveau recherche, publiés ou non, émanant des établissements d'enseignement et de recherche français ou étrangers, des laboratoires publics ou privés.

Comparison Between Voltage and Current Driving Methods of a Micro-Speaker

E. Sturtzer^{a,*}, G. Pillonnet^a, G. Lemarquand^b, N. Abouchi^a

^a*Lyon Institute of Nanotechnology (INL), UMR CNRS 5270,
University of Lyon, Lyon, France – <http://inl.cnrs.fr/>*

^b*Acoustical Laboratory of University of Maine (LAUM), UMR CNRS 6613,
University of Maine, Le-Mans, France – <http://laum.univ-lemans.fr/>*

Abstract

Since its inception, most audio amplifiers control the loudspeaker in voltage. However previous studies highlighted the importance of the loudspeaker control in current. These studies have been done only with large size loudspeakers (bass or midrange loudspeakers) and this is certainly not transposable for the type of loudspeaker in interest i.e. micro-speaker. First of all, this paper describes a model of loudspeaker (voltage driven and also current driven) represented by a comprehensive set of data based on a minimal number of measurements. Simulation results based on these models are presented using single frequency signals such as multi-frequencies signals to compare the two driven methods. At this level of modelling, simulation results show that, contrary to the woofer applications, current driving of micro-speaker does not affect significantly in terms of harmonic distortions, intermodulation distortions and transient behaviour.

Keywords: Micro-speaker, Non-linear modelling, Current-driving, Acceleration, Intermodulation, Transient analysis

1. Introduction

During the last few years, there has been a growing market demand for embedded audio equipment in multimedia devices such as cell phone, smart-phone or tablet PC. In this type of devices, the main challenge is to make the better trade-off between power efficiency, audio quality, acoustical power, integration.

*Principal corresponding author

This document is a collaborative effort (2009–2013 SAIPON project; funding: French National Research Agency).

Email addresses: eric.sturtzer@cpe.fr (E. Sturtzer), gael.pillonnet@cpe.fr (G. Pillonnet), guy.lemarquand@univ-lemans.fr (G. Lemarquand), nacer.abouchi@cpe.fr (N. Abouchi)

Unfortunately, poor sound quality is often synonymous with this kind of product despite more accurate characterization and design method tools [1–4]. Three possibilities exist in order to increase the quality of the audio system: improve audio amplifier performances [5–7], improve loudspeaker design/specification [8–10] and improve the link between them [11]. If we compare the quality of the audio amplifiers (linear & switching) to the quality of the loudspeakers, we can safely say that it is basically on the side of the loudspeaker that there are improvements to be put in place. Micro-speakers are rarely studied in literature [12] despite the wide range of embedded products using this type of loudspeaker. Get better loudspeakers should be a relevant solution to improve the global quality of the system. Despite these works and the technological process improving the linearity, low-cost loudspeakers used in multimedia devices are still highly non-linear. Hence a global approach (i.e. improve the link between loudspeaker and amplifier) might be more effective to this problem and this study will be a great benefit to join both communities: electrical and acoustical.

Usually, one method used to correct the error introduced by the power amplifier is the feedback technique [13]. Voltage driving is the most common technique but it is also possible to impose a current into the loudspeaker voice coil. It would be relevant to enslave the current rather than the output voltage of the amplifier because the force applied to the membrane is directly proportional to the current supplied by the amplifier (when reluctance force is neglected).

Current-feedback audio amplifiers were introduced primarily because they overcome the bandwidth variation, inversely proportional to closed-loop gain, exhibited by voltage-feedback amplifiers. Moreover the current feedback can achieve better slew-rate performance for a given quiescent supply current. It can lead to better dynamic intermodulation distortion performance due to these two previous advantages [14]. The current control also offers better compensation of output filter characteristics especially when a Class-D amplifier is used [15, 16]. Firstly, the amplifiers' transfer with an output filter becomes increasingly unpredictable for loads which are not purely resistive, which is the case for practical loudspeakers. Secondly, the filter suffers from non-linearity (e.g. saturation effect in ferrite). The current feedback can also track the loudspeaker changing for temperature protection or bandwidth optimization [17]. Some mixed mode feedback combined current and voltage controls has been introduced [18, 19] to combine the inherit distortion reduction of current and stability of voltage feedback. Other feedback technique as the motional feedback [20] or negative source impedance [21] improves the over-all response characteristic and reduces the total distortion.

Previous studies [22, 23] highlighted the importance of the loudspeaker control with contentious discussions. [22] measured a difference of $26dB$ in terms of distortions between the current and the voltage control. Unfortunately, these studies have been done but only with large size loudspeaker (bass or midrange loudspeakers) and this is certainly not transposable for the type of loudspeaker in interest (i.e. micro-speaker). [23] claims a great sound improvement by using current mode without indisputable comparison. To conclude, these previous works lead to study deeper the amplifier and loudspeaker coupling in current

mode control for improving the state of the art performance of small volume audio system (e.g. in mobile phone).

The aim of this paper is to confront two control methods by modelling the loudspeaker. For this, we need to correctly model the loudspeaker concerning linearity and transient response of the signal using the model of [24]. An electro-mechano-acoustic model of the loudspeaker (involving a relevant number of nonlinearities), is introduced and will be discussed in the first section. The second section will introduce the purpose of this paper: present two electro-mechanical models to see the impact of the loudspeaker driving methods. The simulations results of these models will be synthesized in the last section and will allow us to conclude on the interest of each driving methods for micro-speaker.

2. Key concept to model a loudspeaker

A loudspeaker is a transducer able to convert electrical energy into acoustic energy. This transformation can be done from different physical principles (capacitive, electrostatic, electro-dynamics). The one who is of interest here is the electro-dynamics principle because it is the principle the most widely used in embedded systems. Extensive research has already been carried out to develop electro-dynamics loudspeaker models [24, 25] and this work is based on these models.

2.1. Different way of modelling the loudspeaker

A figure representing the well-known equivalent electrical circuit of the loudspeaker is presented in Fig. 1. We find all the electrical parameters (R_e the voice-coil resistance, L_e the voice-coil inductance and R_μ the eddy current resistance), the electromechanical coupling is also used (Bl the force factor), the mechanical part (m_m the moving mass, r_m the mechanical resistive losses and c_m the suspension compliance) and the acoustical part (S_d the equivalent area of the piston and $Y_{av/ar}$ the admittances of the acoustic radiation). $u(t)$ and $i(t)$ are the loudspeaker input voltage and current, F the force applied to the diaphragm, $v(t)$ the diaphragm velocity, q_d the diaphragm flow and $p_{1/2}$ the acoustic pressure.

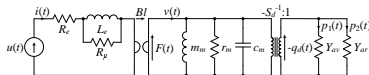


Figure 1: Equivalent electrical circuit of the loudspeaker (electrical, mechanical & acoustic).

A low frequency approximation allows us to simplify the diagram presented in Fig. 1. The radiation resistance (R_{av} & R_{ar}) is far below r_m so it will be neglected and disappears of schematics and equations. But for the mass, we must take into account a radiation mass m_r . The piston is small compared to the wavelength ($ka < 1$) so we obtain a new mass (equal to $m_m + 2m_r$ with

$m_r = 8/3 \times \rho a^3$, ρ the density of air and the radius of the piston). From now on, m_m directly incorporates m_r . As all components are linear at this stage, an analytic resolution can solve the model. The found equivalent circuit of the loudspeaker is Laplace-transformed in equations (1), with x the voice coil displacement.

$$\begin{aligned} u(s) &= R_e i(s) + \frac{R_\mu \times L_e s}{R_\mu + L_e s} i(s) + Bl s x(s) \\ F(s) &= m_m s^2 x(s) + r_m s x(s) + \frac{1}{c_m} x(s) \\ F(s) &= Bl \times i(s) \end{aligned} \quad (1)$$

These equations are time-dependant (we will see in the next section that they also are displacement-dependant) and it will be easier to use a numerical solver. The electro-mechano-acoustic equivalent circuit, Laplace-transformed in equations (1), can also be depicted with a block diagram, shown in Fig. 2.

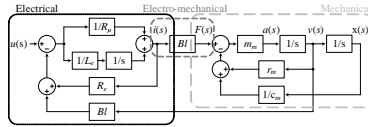


Figure 2: Equivalent block diagram of the loudspeaker.

2.2. Electrodynamics loudspeaker non-linearities presentation

The loudspeaker non-linearities depend on displacement (and on electrical current for the voice coil). For this study, when the input signal applied is a low amplitude signal, the loudspeaker is considered as linear (even if it is not entirely true due to the dependence on current). As presented in Fig. 3, the non-linearities are taken into account for signals of higher amplitude. It is therefore necessary to take into account the dynamics changing of displacement over time to correctly model our system.

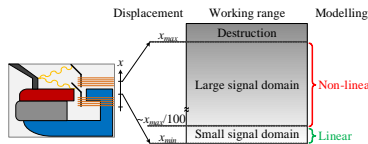


Figure 3: Example of working range function of voice coil displacement.

The three electromechanical parameters most disturbed by the effects of non-linearity are: the compliance of the suspension c_m ; the force factor Bl and the inductance of the coil L_e . Non-linearity data given in this document are all based on measurements using [26] (a measurement bench specifically designed to perform this kind of measures). The Fig. 4 shows an example of measured non-linearities as a function of the position of the membrane.

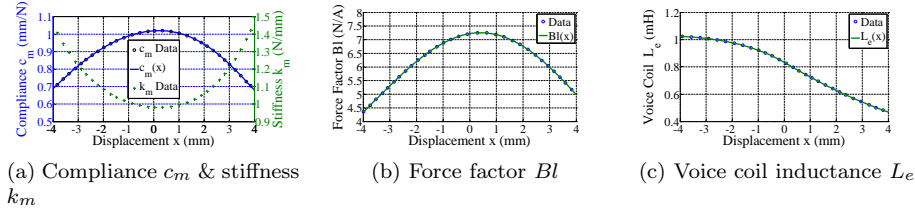


Figure 4: Example non-linearities function of voice coil displacement .

To equate this curve, a polynomial regression (equations (2) with p the polynomial degree) will be used in the non-linear Matlab model which will be presented in section 3.1.

$$\begin{aligned}
 c_m(x) &= c_{m_0} + \sum_{n=1}^{n=p} (c_{m_n} x^n) \\
 Bl(x) &= Bl_0 + \sum_{n=1}^{n=p} (Bl_n x^n) \\
 L_e(x) &= L_{e_0} + \sum_{n=1}^{n=p} (L_{e_n} x^n)
 \end{aligned} \tag{2}$$

Now observe the variation of the inductance of the coil. We define the coefficient of magnetic induction of the coil $L(t)$ by the ratio of the magnetic flux $\Phi(t)$ and the current $i(t)$ who creates it; $L(t) = \Phi(t)/i(t)$. The difference of potential appearing thanks to the auto-inductive effect across the linear coil is $u_L(t) = d\Phi(t)/dt$. In other words, $u_L(t) = L \times di_L(t)/dt$, whereas in the case of the loudspeaker, equation (3) is used to represent the non-linear difference of potential. This equation is divided in two parts, the first is the linear part (with constant inductance replaced by position dependent coil) and the second part can be considered as a voltage generator function of voice coil displacement and time depending.

$$u_L(t, x(t)) = \frac{i_L(t) + L_e(x(t))}{dt} = L_e(x(t)) \frac{di_L(t)}{dt} + i_L \frac{L_e(x(t))}{x(t)} \frac{dx(t)}{dt} \tag{3}$$

With u_L voice coil voltage (V)
 i_L voice coil current (A)
 x coil displacement (m)
 L_e voice-coil inductance (H)

Looking at the magnetic energy in an inductor, $W_{mag} = 1/2 \times \Psi^2(t)/L_e = 1/2 \times L_e \times i_L^2(t)$. Due to the principle of conservation of energy, the magnetic energy is proportional to the square of the current. This energy cannot abruptly change and will remain constant. In the case of a decrease of the inductance

value and of a constant current, the excess of energy provides a force that tends to pull the coil in its previous position. Equation (4) shows the conversion of energy that will force the coil to move along the axis of displacement x . This phenomenon of reluctance force will be added in the non-linear model of the loudspeaker.

$$F_r(x(t), i_L(t)) = -\partial_\xi W_{mag}(t) \equiv \frac{1}{2} i_L^2(t) \frac{dL_e(x)}{dx} \quad (4)$$

With	F_r	reluctance force (N)
	ξ	elongation (m)
	W_{mag}	magnetic energy (J)
	i_L	voice coil current (A)
	x	coil displacement (m)
	L_e	voice-coil inductance (H)

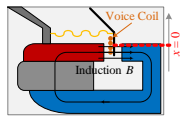
All these phenomena (i.e. $Bl(x)$, $c_m(x)$ & $L_e(x, i_L)$) used in equations (5a) & (5b) will be added in the non-linear model of the loudspeaker. To add these data (as in Fig. 4), polynomial regressions will be used coupled with equations given in (2) and (4). Needing polynomial regressions, a numerical tool will be required to model the loudspeaker. Section 4 will develop this implementation.

$$u(t) = R_e i(t) + \frac{R_\mu L_e(x, i_L) \frac{\partial i_L(t)}{\partial t}}{R_\mu + L_e(x, i_L) \frac{\partial i_L(t)}{\partial t}} i(t) + Bl(x) v(t) \quad (5a)$$

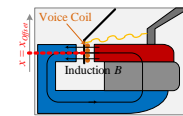
$$F(t) = Bl(x) \times i(t) = m_m a(t) + r_m v(t) + \frac{1}{c_m(x)} x(t) - \frac{1}{2} i_L^2(t) \frac{dL_e(x)}{dx} \quad (5b)$$

2.3. Voice coil offset correction

Another phenomenon to add to the model is the adjusting of the coil's rest position. If we look at Fig. 5 we can see that the rest position of the coil in Fig. 5a is not centred inside the inductive field B and Fig. 5b shows the position it should take. We will see in section 4.2 the importance to add this coil shift in the modelling.



(a) Rest position



(b) Voice coil offset

Figure 5: Adjusting coil's rest position.

2.4. Impedance (modulus & phase vs. frequency)

For audio amplifier designers, the loudspeaker impedance is often modelled by a resistor (coupled to an inductance in the best case). This is far from enough. Indeed, to properly design an audio amplifier, the designer must take into account a load correlated with the amplifier to match with provide power. The impedance or voltage to current transfer function is presented in equation (6).

$$Z(s) = (R_e + Z_e(x)) \frac{s^2 + \frac{Bl^2(x) + (R_e + Z_e(x)) \cdot r_m}{(R_e + Z_e(x)) \cdot m_m} s + \frac{1}{c_m(x) \cdot m_m}}{s^2 + \frac{r_m}{m_m} s + \frac{1}{c_m(x) \cdot m_m}} \quad (6)$$

$$\text{where } Z_e(x) = \frac{R_\mu \cdot L_e(x, i_L) \cdot s}{R_\mu + L_e(x, i_L) \cdot s}$$

Fig. 6 is an example of electric impedance. We can clearly see that the impedance modulus is not a horizontal line as should be the case for pure resistance. In fact, usually, this loudspeaker would be symbolized by a resistance of 32Ω . But if you look at what happens at the resonance frequency (where the phase angle is zero and magnitude is maximum), we have an impedance rise reaching a value of 37.6Ω (thermal compression). The current consumed to drive the loudspeaker in this frequency range will be lower (to keep the same acoustic level) and the output power of the audio amplifier will also be lower. $|Z|$ will be useful in the calculation of the input current (to be proportional to the input voltage at a specific frequency).

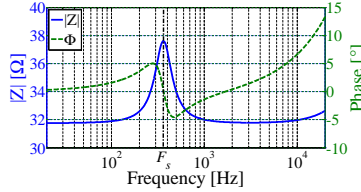
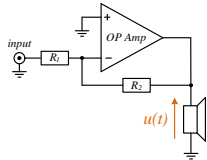


Figure 6: Electric impedance modulus (—) and phase angle (···) vs. frequency of the loudspeaker.

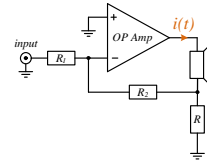
By directly driving the loudspeaker in current, this phenomenon of impedance rise would be less disturbing. The force applied to the membrane is directly proportional to current multiplied to the force factor. The next sections will show that a more complex argumentation is needed to put in place a rigorous comparison between the two driving modes.

3. Modelling the loudspeaker using voltage / current driving principle

Voltage driving is the common technique (i.e. control $u(t)$) but it is also possible to impose a current $i(t)$ into the loudspeaker voice coil as presented in Fig. 7.



(a) Voltage driving principle



(b) Current driving principle

Figure 7: Simplified principle of voltage (7a) and current (7b) driving of loudspeakers.

To characterize its behaviour, the loudspeaker is modelled in Matlab coupled with Simulink environment. The next subsection will present the model of the loudspeaker controlled by voltage or current.

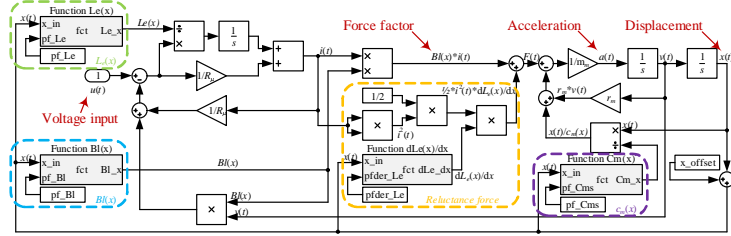
3.1. Presentation of the model

The implementation of the Simulink model contains all the parameters discussed previously. The graphical block diagramming given in Fig. 8a & 8b correspond respectively to the loudspeaker controlled by voltage and by current. From this model it is possible to visualize the loudspeaker variable (current, force factor, acceleration, displacement, etc.). To include non-linearities, blocks called S-Function coupled with polynomial regressions are used to add non-linearities. If we consider the example of the force factor $Bl(x)$, as we saw in Fig. 2, this parameter depends on its position $x(t)$. A polynomial regression is extracted from the data to be used in the block “Function $Bl(x)$ ” Function that generates the value of the force factor considering its current position x . The same principle is applied to $c_m(x)$ and to $L_e(x)$. The last non-linear parameter presented in equation (4) is the derivative of the voice coil inductance relative to its position. Its polynomial regression has been derived before being coupled with its position in the block “Function $dL_e(x)/dx$ ”.

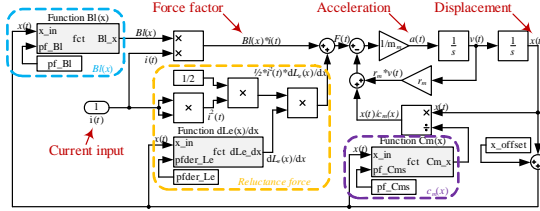
Note that the diagram presented in Fig. 8b shows that there are a number of parameters which will be simplified compared to the diagram shown in Fig. 8a. Driving by current removes certainly non-linearities but compared to the complexity that it might bring to the electronics controlling the loudspeaker, is this difference really significant? A comparative study with simulation results will be developed in the next section of this paper.

3.2. Model validation

To test the viability of the model, a comparison with [22] has been performed. The parameters for example drive unit (bass-midrange loudspeaker) are given in Appendix A. Non-linear parameters function of displacement used are extracted from the curves presented by P. G. Mills and M. J. Hawksford in [22, Fig.1]. The results found, using the non-linear parameters of their loudspeaker in our model (neglecting the reluctance force), are similar to those of its publication.



(a) Voltage driving block diagram



(b) Current driving block diagram

Figure 8: Simulink block diagram of the model of the non-linear loudspeaker.

4. Results of the comparison between voltage and current driving

To get a large range of comparison, various types of electrodynamic loudspeakers will be modelled: a woofer, a bass-midrange, a micro-speaker and a headphone loudspeaker (linear parameter in Appendix A). A more detailed study will be carried out on the micro-speaker. As an example of non-linearities, the parameters of the micro-speaker are given in Appendix B. Audio comparison (especially focused on the acceleration of the membrane) is performed in terms of distortion, intermodulation study and finally, a transient signal is also used to have a wide representative sample of the various signals that can be injected into a loudspeaker.

4.1. Acceleration response

Typically, the output of interest is the diaphragm acceleration $a(s)$, due to its proportionality to the sound pressure (always assumed to be with an ideal piston mode). For high frequencies, piston mode is not completely correct (presence of modes of the membrane) but this hypothesis is sufficient because the control (in current or voltage) will never improve the non rigidity of the membrane. Equations (7a) & (7b) are respectively acceleration magnitude of the voltage control and of the current control.

$$Z_{a/u}(s) = \frac{\frac{Bl(x)}{(Z_e(x)+R_e)m_m} s^2}{s^2 + \left(\frac{Bl^2(x)}{(Z_e(x)+R_e)m_m} + \frac{r_m}{m_m} \right) s + \frac{1}{c_m(x)m_m}} \quad (7a)$$

$$Z_{a/i}(s) = \frac{Bl(x) c_m(x) s^2}{m_m c_m(x) s^2 + r_m c_m(x) s + 1} \quad (7b)$$

An example is the bode plot of the acceleration magnitude shown on Fig. 9 based on a micro-speaker (characteristics in Appendix A). Near the resonance frequency, this figure shows a greater overshoot for $Z_{a/i}$ than for $Z_{a/u}$. Phenomenon due to the total quality factor (electrical + mechanical) which is higher for the voltage control.

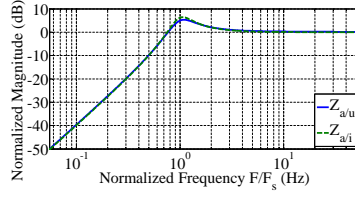


Figure 9: Bode plot of a micro-speaker input voltage (—) & input current (···) to diaphragm acceleration magnitude.

4.2. Voice coil offset – Assessing the asymmetry of the $Bl(x)$ curve

As presented in section 2.3 and in Fig. 8, x_{offset} represent the coil's offset due to the asymmetry (relative to the voice coil rest position). The target to use x_{offset} in the model, is to keep the force factor value as symmetrical as possible. As an example, Fig. 10a shows a simulation with a membrane peak amplitude $x_{ac} = 0.1mm$ using $x_{offset} = 0mm$ and Fig. 10b shows a simulation with the same amplitude x_{ac} but with x_{offset} equal to the displacement position of the maximum of Bl (in this case $x_{offset} \approx 0.15mm$). We observe a maximal Bl variation $\Delta_{Bl} = 12\%$ (between x_{max} and x_{min}) in Fig. 10a and a $\Delta_{Bl} = 1.1\%$ in Fig. 10b. This example validates the benefits of using a system to adjust the position of the coil (notice that IEC standard 62458 recommends a $\Delta_{Bl} < 5\%$). Due to a possible high variation of Δ_{Bl} , it will be necessary to incorporate this phenomenon into the model (it applies for both control – voltage & current).

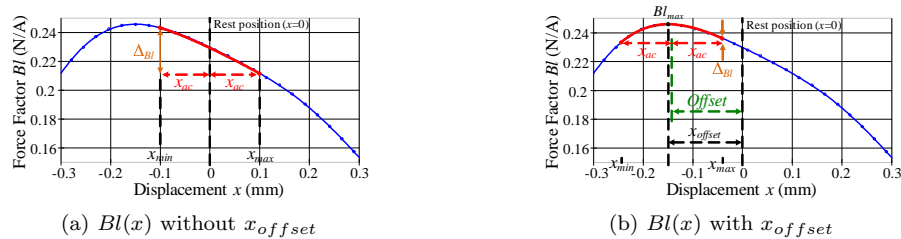


Figure 10: Impact of the x_{offset} on the $Bl(x)$.

What is also interesting to note is that there is an improvement in the symmetry of the field for high amplitude (improvement compared to the forced position x_{offset}). Indeed, in Fig. 11 which shows the curve of the average value of the peak-peak amplitude of the displacement, one sees an improvement in

the asymmetry which is due to the field (offset tends to get closer to the rest position).

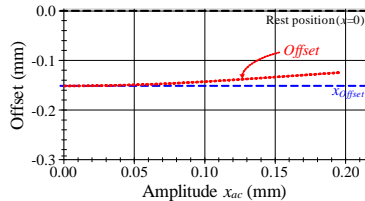


Figure 11: Displacement offset function of displacement amplitude

4.3. Distortion analysis

4.3.1. Electrical distortion analysis

If distortions occur in the current $i(t)$ (see Fig. 8a), we will find them directly in the force applied to the membrane (as seen in equations (5)). Fig. 12 shows a THD level of $\approx -47dB$ (simulated and measured for a current in the coil of $20mA$). This THD level is not a negligible value. This first result could guide us directly towards the choice of a current driving, i.e. no current distortions, but a supplementary study is necessary.

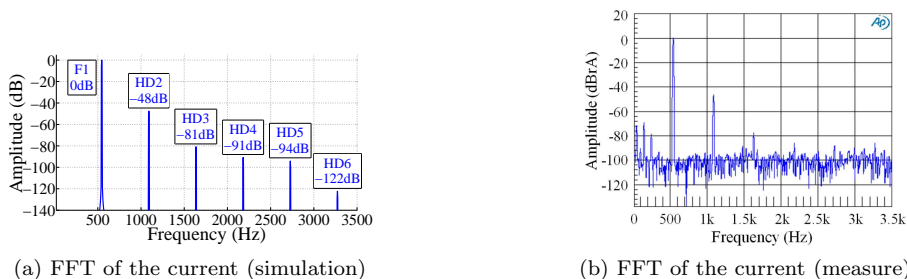


Figure 12: FFT simulation and measurement of $i(t)$ in voltage control.

Note that Fig. 12a and Fig. 12b show a second time the model viability. In fact, if Fig. 12a had been standardized so as Fig. 12b, we end up with two curves almost identical.

4.3.2. THD simulation method

Different fundamental frequencies ($F1$) have been chosen for each loudspeaker simulation. To scan a wide audio frequency range, the simulation is carried out at $100Hz$, $1kHz$ and $10kHz$ (voice frequency range $[80Hz \rightarrow 14kHz]$). To these previous frequencies, measures at the resonance frequency (F_s) and at twice the resonance frequency are added. We choose to simulate at these frequencies because non-linearities introduce distortion by large displacement and

this is the case around the resonance frequency. To detect distortions in the signal, a frequency domain analysis is necessary.

The second point of interest is the signal amplitude. To compare the two driving modes, equivalent electrical signals must be injected to produce an equivalent acoustical power level. The current amplitude (i_{RMS}) is fixed, and then to know the value of the equivalent voltage amplitude (u_{RMS}), generalized Ohms law has been used with the non-linear impedance Z (cf. equation (6)). After simulation, it appears that the amplitude of the displacement (which is proportional to the acoustical power) of the two models is identical. In other words, the comparison is performed with the same conditions. Note that ideal current and voltage sources are used to model the audio amplifier output signal (hypothesis which will be validated later).

4.3.3. Acoustical THD results

Table 1 contains the THD measurements of the different loudspeaker simulations with both driving methods. We note that there are more distortions at low frequencies (especially around F_s). This is due to a more important displacement at these frequencies (for the same acoustical output power). By observing the relative difference Δ THD between the distortion attenuation of a loudspeaker controlled by voltage compared to the current driven loudspeaker, it shows that this difference is significant for the woofer and also for the bass-midrange loudspeaker. It is less relevant for the micro-speaker and for the headphone loudspeaker (for all fundamental frequencies used in this test).

Loudspeaker↓ \ Frequencies →	100Hz	1kHz	10kHz	F_s	$2 \times F_s$
Woofer ($F_s \approx 38Hz$)	-49.4 -53.5	-66.9 -66.2	-56.9 -72.1	-12 -21.2	-44.7 -50
Bass-midrange ($F_s \approx 48Hz$)	-59.8 -63.6	-73.2 -75.5	-62.6 -82	-29.6 -26.5	-58.9 -63.7
Microspeaker ($F_s \approx 363Hz$)	-12 -11.7	-63.5 -63.4	-79.2 -79.3	-24.2 -24	-54.1 -53.9
Headphone ($F_s \approx 429Hz$)	-20.2 -20	-49.4 -49.3	-68.2 -68.5	-29.5 -28.9	-45.8 -45.7

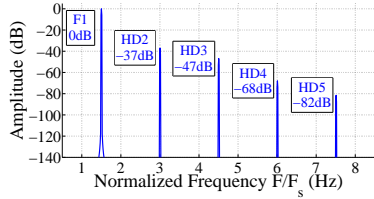
Legend: left data \rightarrow THD (dB) in voltage driving & right data \rightarrow THD (dB) in current driving.

Table 1: THD data from different type of loudspeakers according to the frequencies.

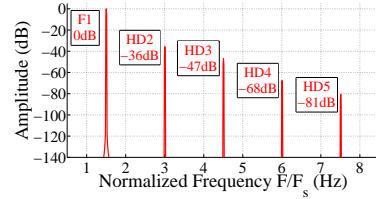
4.3.4. Influence of voltage or current driving on non-linear parameters which affects the THD

Each non-linear parameter impacts the distortions. To show these phenomena, a relevant signal for a type of loudspeaker is chosen: a sinusoidal signal with $F1 = 1.5 \times F_s$ is applied to the micro-speaker which is under interest. For a current amplitude $i_{RMS} = 20mA$ and with $|Z_{F1}| \approx 33\Omega$ (the impedance modulus at the fundamental frequency), the micro-speaker will be driven by an electrical power near $13mW$ (a high but acceptable value for this type of loudspeaker).

For the voltage controlled model, $v_{RMS} = i_{RMS} \cdot |Z_{F1}| \approx 660mV$. The details of the harmonic distortion spectrum of the micro-speaker acceleration are presented in Fig. 13 (simulation performed with all the non-linear parameters). The level of $THD \approx -36dB \cong 1.6\%$ ($-36.6dB$ for voltage and $-35.4dB$ for current driving) is huge compared to the value required in standard audio amplifier specification for embedded systems (0.1% in the worst case). Therefore we were right to consider the amplifier as ideal in the model presented in Fig. 8 (but that does not mean that this parameter should be underestimated in audio amplifiers). We can ask ourselves what is the impact (if there is one) of voltage or current driving on each parameter taken separately. Fig. 13 could serve as a reference to quantify the contribution of the non-linear parameters taken separately. But rather than carrying out this study based on the harmonic distortion, it seems more appropriate to make the intermodulation distortion analysis as presented in section 4.4.



(a) Harmonic distortion spectrum of the micro-speaker acceleration in voltage control



(b) Harmonic distortion spectrum of the micro-speaker acceleration in current control

Figure 13: Harmonic distortion spectrum of the micro-speaker acceleration simulate with $Bl(x)$, $c_m(x)$ & $L_e(x, i_L)$.

4.4. Intermodulation distortions

Intermodulation distortion (IMD) is the effect of non-linearity for an excitation which is the sum of a high frequency $F2$ and of a low frequency component $F1$. This effect consists in the component modulation of the response of the frequency $F2$ to the frequency $F1$, manifesting itself by side bands of frequencies $F2 + F1$ ($= IMD2$), $F2 + 2 \cdot F1$ ($= IMD3$), etc., as presented in Fig. 14.

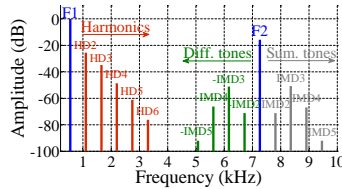


Figure 14: Example of IMD spectrum of the micro-speaker acceleration.

Table 2 show the voice sweep distortion results with a two-tone stimulus applied to the two models of the micro-speaker. $F1 = 1.5 \cdot F_s$ ($= 545Hz$) represents an instrument tone and $F2 = 5 \cdot F_s \rightarrow 20 \cdot F_s$ ($\equiv 1.8kHz \rightarrow 7.3kHz$) represents the voice tone.

$F2 = 5 \cdot F_s$	HD_2		HD_3		$-IMD_3$		$-IMD_2$		$F2$		$+IMD_2$		$+IMD_3$	
	-24.6	-24.3	-33.8	-33.3	-54	-53.7	-56.9	-56.9	-15.8	-15.9	-57	-56.9	-55.6	-55.4
$F2 = 10 \cdot F_s$	HD_2		HD_3		$-IMD_3$		$-IMD_2$		$F2$		$+IMD_2$		$+IMD_3$	
	-24.6	-24.3	-33.8	-33.3	-52.5	-52.3	-85.3	-86	-16.1	-16.2	-81	-81	-52.6	-52.5
$F2 = 15 \cdot F_s$	HD_2		HD_3		$-IMD_3$		$-IMD_2$		$F2$		$+IMD_2$		$+IMD_3$	
	-24.6	-24.3	-33.8	-33.3	-52.1	-52	-74.2	-73.8	-16.1	-16.3	-74.2	-73.8	-52.2	-52
$F2 = 20 \cdot F_s$	HD_2		HD_3		$-IMD_3$		$-IMD_2$		$F2$		$+IMD_2$		$+IMD_3$	
	-25.3	-25.1	-35.2	-34.7	-52.6	-52.5	-71.8	-71.6	-16	-16.1	-71.9	-71.6	-52.6	-52.5

Legend: left data \rightarrow amplitude (dB) in voltage driving & right data \rightarrow amplitude (dB) in current driving.

Table 2: Voice sweep distortion results with a two-tone stimulus.

4.4.1. Influence of voltage or current driving on non-linear parameters which affects the THD and IMD

Fig. 15 shows a sample of measurement, of a two-tone stimulus applied to the two models of the micro-speaker (using x_{offset}). Each sub-figure represent a simulation with respectively all non-linear parameters, only $Bl(x)$, only $c_m(x)$, only $L_e(x)$ and finally only the reluctance force phenomenon. As presented in section 4.2, it is observed in the temporal simulations (Fig. 15a) that there is a displacement offset. This is easily explained with the curve of $Bl(x)$ presented in Fig. 15b which is not centred on zero but centred around $x_{offset} \approx 0.15mm$.

In Fig. 15b, the resulting signal is obtained with the previous input conditions but *only* with Bl function of x . A comparison between measurements is presented in table 3. Some of these values function of $Bl(x)$ (e.g. $-IMD2$ & $IMD2$) are bigger than the measure functions of all parameters. Non-linearities may compensate each other but it is out of scope. With such a distortion level, we can easily understand that the force factor has a major impact on non-linearity of the system. It can be seen by comparing the different harmonics that the odd harmonics are much affected than the even harmonics. We see that $HD3$ or $\pm IMD3$ is much more affected with the compliance non-linearities. If we look at what happens in terms of voltage or current driving of the loud-speaker, we observe no significant difference between the two control techniques.

As with only the force factor, the distortion level is high when only $c_m(x)$ is taken into account such as in Fig. 15c. It affects both the even/odd harmonics. A slight difference is present between the current and the voltage control. It could be easily predicted because the control has no impact on the previous equations of $Z_{a/u(s)}$ & $Z_{a/i(s)}$ (cf. equations 7a and 7b).

For the micro-speaker under test, the influence of the voice-coil inductance vs. displacement is insignificant for the two driving methods as we can see in

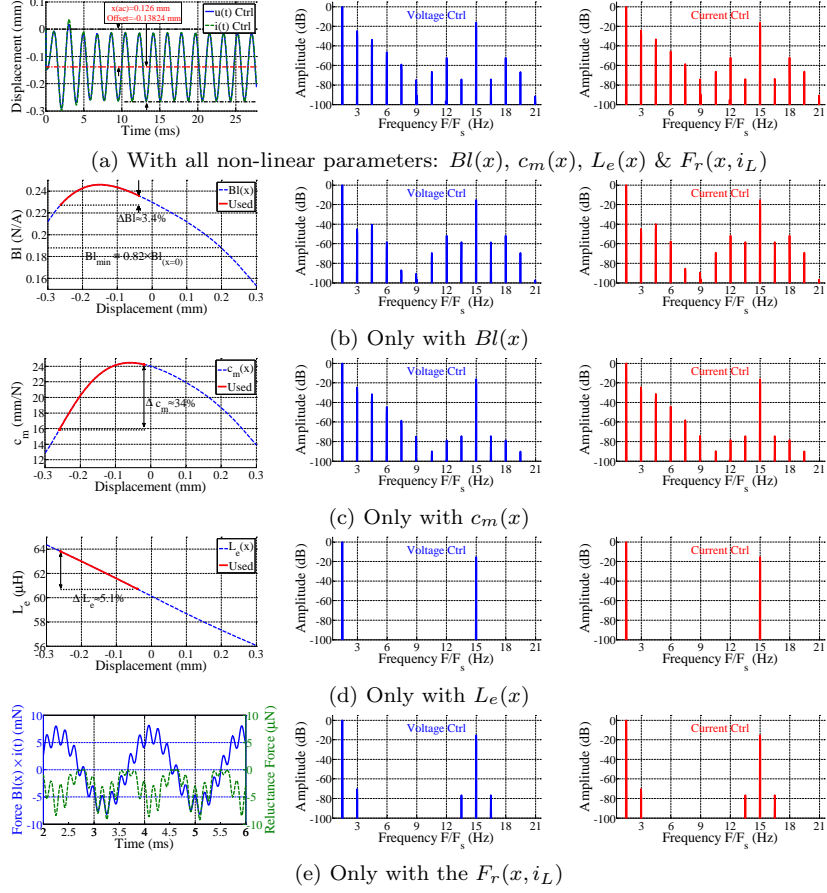


Figure 15: Intermodulation spectrum of $a(t)$ of the micro-speaker. For $i(t) = \sqrt{2} \cdot I_1 \sin(2\pi F_1 t) + \sqrt{2} \cdot I_2 \sin(2\pi F_2 t)$, with $I_1 = 20mA$ ($0dB$); $I_2 = I_1/4$ ($\equiv -12dB$); $F_1 = 1.5 \cdot F_s$ and $F_2 = 15 \cdot F_s$.

Fig. 15d. Its impact seems minimal compared to the force factor $Bl(x)$ and the compliance $c_m(x)$. The fact that micro-speaker is controlled by current removes the dependency between L_e and displacement. Despite this difference, the low value of the coil ($L_e \approx 60\mu H$) coupled with its small variation ($\Delta L_e \approx 5\%$) does not allow to find a difference between the two control principles.

For Fig. 15e, only the reluctance force phenomenon has been used in the model (linear Bl , c_m and L_e). As it was presented in the equation 4, we saw the emergence of a reluctance force which also disturbs the signal (see $HD2$, $-IMD2$ & $IMD2$ in the figure). But these distortions are negligible compared to the THD level of $Bl(x)$ or $c_m(x)$.

The distortions due to the non-linear inductance are less important at low frequencies, but more important in high frequency range [27]. Note that for

the same reasons as for the voice coil effect (low value of L_e coupled with its small variation), control in voltage or in current does not affect distortions due to reluctance effect.

	All non-linearities		Only $Bl(x)$	
	Voltage	Current	Voltage	Current
<i>HD2</i>	-24.6	-24.3	-45	-44.7
<i>HD3</i>	-33.8	-33.3	-40.5	-39.9
<i>-IMD3</i>	-52.5	-52.3	-51.8	-51.7
<i>-IMD2</i>	-85.3	-86	-58.4	-58.4
<i>F2</i>	-16.1	-16.2	-15.2	-15.3
<i>IMD2</i>	-81	-81	-58.4	-58.4
<i>IMD3</i>	-52.6	-52.5	-51.8	-51.7

Table 3: IMD measurement (in dB) – Comparison between model using all non-linear parameters and using only Bl function of displacement.

4.4.2. Intermodulation simulations conclusion

As expected, the most perturbing parameter in terms of IMD is the force factor. Bl mainly affects the even-order harmonic and is disturbing all along the frequency range. Compliance affects more the odd-order harmonics. That is the reason why the second harmonic is lower and the third higher than for $Bl(x)$ in Fig. 15. In terms of IMD, the compliance does not affect significantly. In fact, this mechanical parameter is more disturbing around the resonance frequency (more impact on HD than Bl). The parameter which could make the difference between voltage or current driving is the voice coil inductance. Unfortunately, as presented in Fig. 15d, $L_e(x)$ has no impact ($\leq 100dB$).

Harmonic distortions and intermodulation distortions are only indicators of the effects of audio quality. Observing the spectra will not be sufficient to show how the loudspeaker behaves during transient conditions. The next section will solve this lack.

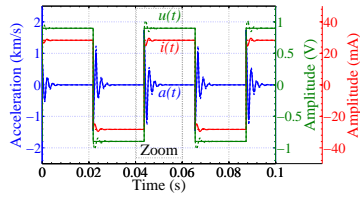
5. Transient analysis

Transient analysis study is particularly important for strong variations (e.g. for a peak value). In other words, this analysis is useful when critical acceleration or natural resonances are encountered (which is possible with audio signals).

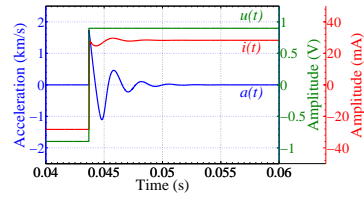
5.1. Step response

Fig. 16 shows a step response of the voltage, the current and the acceleration function of time and Fig. 16a for the two controls (Fig. 16b–16c are respectively the zoom of voltage control and current driving). It is also a good way to observe the quality factor of the micro-speaker. As the electrical quality factor ($Q_{es} = 11$) is bigger than the mechanical quality factor ($Q_{ms} = 2$), the total

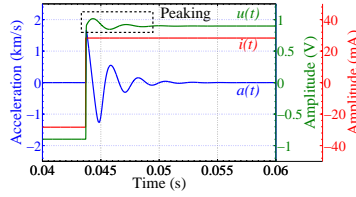
quality factor ($Q_{ts} = 1.7$) mainly depends on the mechanical part. For the current control, the total quality factor depends only on the mechanical part ($Q_{ts} = Q_{ms} = 2$). As the two Q_{ts} are quite close, the difference in acceleration between the two controls is therefore not very important. Note that for the current control (Fig. 16c), there is a peaking for the voltage. As voltage is limited in amplitude in embedded systems, one needs to be careful.



(a) Voltage control (–) & current control (···).



(b) Zoom of the voltage control



(c) Zoom of the current control

Figure 16: Transient plot of the voltage $u(t)$, the current $i(t)$ and the acceleration $a(t)$.

5.2. Spectrogram (waterfall)

If a white noise is applied and abruptly stopped e.g. Fig. 17a, the spectrogram will allow us to see a possible dragging [28]. The dragging is a badly controlled inertia of the membrane of the loudspeaker, which consequence is an artificial extension of sound, that may impair the quality of the transient audio signal. It is an important representation of audio data because human hearing is based on a kind of real-time spectrogram. The spectrogram can be defined as an intensity plot (in dB) of the Short-Time Fourier Transform (STFT) magnitude. The STFT is simply a sequence of FFTs of windowed data segments, where the windows are usually allowed to overlap in time. Waterfall results (always without membrane modes) are presented in Fig. 17b & 17c. The two dragging are almost equivalent in terms of amplitude, frequency and time length.

6. Conclusion

The use of voltage feedback or current control techniques is discussed in this article for a micro-speaker. A reliable model of loudspeaker is proposed,

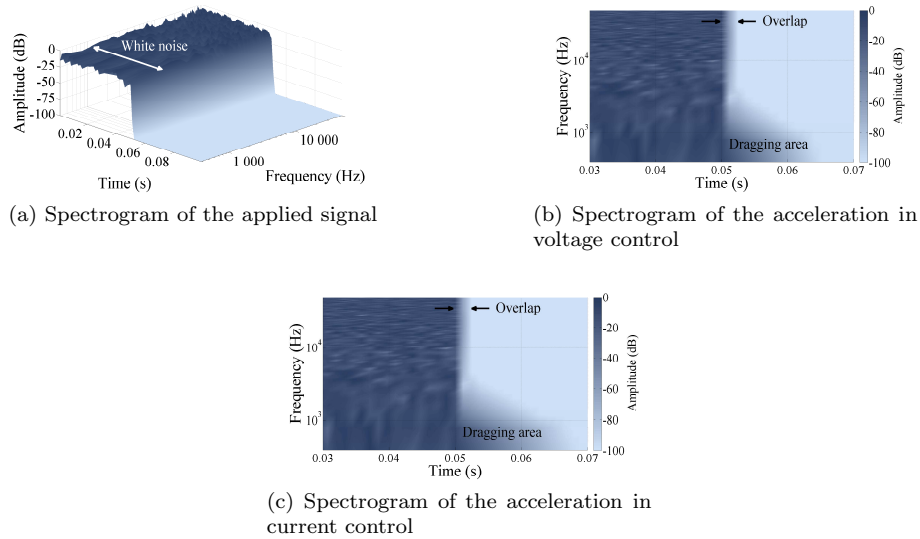


Figure 17: Waterfall – Spectrogram results.

associated with both control techniques. The model is based on a minimal number of equations and measurements involving major non-linear parameters of the loudspeaker under test. Different results based on harmonic distortions, intermodulation distortion simulations and transient analysis using voltage or current driving loudspeakers are presented. In current control, a more important effect of peaking can be disturbing to the acceleration of the membrane during transient response. Simulation results show that current driving does not affect significantly in terms of distortion (HD & IMD) the micro-speaker under test. In terms of transient analysis, due to the high electrical quality factor of the micro-speaker, the current control method does not impact significantly the quality of audio reproducing chain. For micro-speakers and at this level of modelling, the commonly used feedback technique seems to be still a good control technique to drive micro-speaker but the current driving could be an alternative solution.

References

- [1] A. J. M. Kaizer, Modeling of the nonlinear response of an electrodynamic loudspeaker by a volterra series expansion, *JAES* 35 (6) (1987) 421–433.
- [2] W. Klippel, Dynamic measurement and interpretation of the nonlinear parameters of electrodynamic loudspeakers, *JAES* 38 (12) (1990) 944–955.

- [3] R. Ravaud, G. Lemarquand, T. Roussel, Time-varying non linear modeling of electrodynamic loudspeakers, *Applied Acoustics* 70 (3) (2009) 450–458.
- [4] W. Klippel, J. Schlechter, Fast measurement of motor and suspension nonlinearities in loudspeaker manufacturing, in: *AES Convention 127*, 2009.
- [5] G. Pillonnet, R. Cellier, E. Allier, N. Abouchi, A. Nagari, A topological comparison of pwm and hysteresis controls in switching audio amplifiers, in: *IEEE APCCAS Conference*, 2008, pp. 668–671.
- [6] P. Russo, F. Yengui, G. Pillonnet, T. Sophie, N. Abouchi, Switching optimization for class-g audio amplifiers with two power supplies, *Journal of Circuits and Systems*, Scientific Research Publishing 3 (1) (2012) 90–98.
- [7] E. Sturtzer, G. Pillonnet, A. Huffenus, N. Abouchi, F. Goutti, V. Rabary, Improved class-k amplifier for headset applications, in: *IEEE NEWCAS Conference* 8, 2010.
- [8] B. Merit, G. Lemarquand, V. Lemarquand, Performances and design of ironless loudspeaker motor structures, *Applied Acoustics* 71 (6) (2010) 546–555.
- [9] M. Erza, G. Lemarquand, V. Lemarquand, Distortion in electrodynamic loudspeakers caused by force factor variations, *Archives of Acoustics* 36 (4) (2011) 873–885.
- [10] G. Lemarquand, R. Ravaud, I. Shahosseini, V. Lemarquand, J. Moulin, E. Lefevre, Mems electrodynamic loudspeakers for mobile phones, *Applied Acoustics* 73 (4) (2012) 379–385.
- [11] E. Sturtzer, G. Pillonnet, N. Abouchi, F. Goutti, System approach to avoid audio amplifier oversizing in mobile phone application, in: *AES Conference* 43, 2011.
- [12] T. Matsumura, S. Saiki, K. Sano, S. Usuki, Ultra-thin micro-loudspeaker using oblique magnetic circuit., in: *AES Convention 124*, 2008.
- [13] A. Huffenus, G. Pillonnet, N. Abouchi, F. Goutti, V. Rabary, R. Cittadini, A high psrr class-d audio amplifier ic based on a self-adjusting voltage reference, in: *ESSIRC Proceedings*, 2010, pp. 118–121.
- [14] A. Mark, A current-feedback audio power amplifier, in: *AES Convention* 88, 1990.
- [15] P. Van Der Hulst, A. Veltman, R. Groenenberg, An asynchronous switching high-end power amplifier, in: *AES Convention* 112, 2002.
- [16] K. M. Cho, W. S. Oh, W. S. Chung, H. J. Kim, A new class-d stereo audio amplifier using direct speaker current control, in: *IEEE PESC Conference* 35, Vol. 2, 2004, pp. 1308–1310.

- [17] A. Bright, Tracking changes in linear loudspeaker parameters with current feedback, in: AES Convention 115, 2003.
- [18] P. Adduci, E. Botti, E. Dallago, G. Venchi, Pwm power audio amplifier with voltage/current mixed feedback for high-efficiency speakers, *IEEE Transactions on Industrial Electronics* 54 (2) (2007) 1141–1149.
- [19] J. J. Hench, J. Comparetto, Mixed-mode (current-voltage) audio amplifier, Patent, US 7053705 (5 2006).
- [20] E. De Boer, Theory of motional feedback, *IRE Transactions on Audio* 9 (1) (1961) 15–21.
- [21] M. J. Turner, D. A. Wilson, The use of negative source impedance with moving coil loudspeaker drive units: A review and analysis, in: AES Convention 122, 2007.
- [22] P. G. Mills, M. J. Hawksford, Distortion reduction in moving-coil loudspeaker systems using current-drive technology, *JAES* 37 (3) (1989) 129–148.
- [23] E. Merilainen, *Current-Driving of Loudspeakers: Eliminating Major Distortion and Interference Effects by the Physically Correct Operation Method*, Ed. Createspace, ISBN 1450544002, 2010.
- [24] R. H. Small, Closed-box loudspeaker systems-part 1: Analysis, *JAES* 20 (10) (1972) 798–808.
- [25] R. Ravaud, G. Lemarquand, T. Roussel, V. Lemarquand, Ranking of the nonlinearities of electrodynamic loudspeakers, *Archives of Acoustics* 35 (1) (2009) 49–66.
- [26] W. Klippel, R & d system – based on standard iec 62458 (2011).
- [27] B. Merit, V. Lemarquand, G. Lemarquand, A. Dobrucki, Motor nonlinearities in electrodynamic loudspeakers: Modelling and measurement, *Archives of Acoustics* 34 (4) (2009) 579–590.
- [28] S. Loutridis, Resonance identification in loudspeaker driver units: A comparison of techniques, *Applied Acoustics* 66 (12) (2005) 1399–1426.

Appendix A. Electrodynamics loudspeakers parameters (Table A.1)

Parameter	Woofers	Bass-midrange	Micro-speaker	Headphone	Unit
R_e	5.37	7	31.75	30.54	Ω
$L_{e(x=0)}$	0.83×10^{-3}	1.04×10^{-3}	0.06×10^{-3}	0.15×10^{-3}	H
R_μ	3.73	1	0.05	0.37	Ω
$Bl_{(x=0)}$	7.27	7.8	0.23	0.64	N/A
r_m	1.09	2.43	9×10^{-3}	117×10^{-3}	kg/s
m_m	17.11×10^{-3}	18.3×10^{-3}	8×10^{-6}	109×10^{-6}	kg
$m_{m(x=0)}$	1.02×10^{-3}	0.6×10^{-3}	24×10^{-3}	12.6×10^{-3}	m/N

Table A.1: Table settings for the different type of loudspeakers.

Appendix B. Micro-speaker non-linear parameters (Table B.2)

n	0	1	2	3	4	5	6
Bl_n	0.23	-164.71	-1.6×10^6	649.9×10^6	-5.968×10^{12}	1.066×10^{15}	21.4×10^{18}
c_{m_n}	24×10^{-3}	-14.07	-887×10^3	322.5×10^6	-862.4×10^9	-1.63×10^{15}	5.97×10^{18}
L_{e_n}	60.1×10^{-6}	-14.6×10^{-3}	0.61	13.1×10^3	6.52×10^6	-51.86×10^9	-44.23×10^{12}

Table B.2: Coefficients of the non-linear parameters of the micro-speaker.